Chlorofluoromethanes in the Deep Equatorial Atlantic Revisited

C. Andrié

LODYC Laboratoire d'Océanographie DYnamique et de Climatologie, CNRS/ORSTOM/Université Paris 6, Tour 14 - 2° ét., 4 place Jussieu, Case 100, 75252 Paris Cedex 05, FRANCE

Abstract: CFM (CCl_3F or *freon* F-11 and CCl_2F_2 or *freon* F-12) measurements were made on board the R.V. Atalante as part of a quasi-synoptic survey of the tropical Atlantic Ocean. The work was carried out during the CITHER 1 cruise, part of the French CITHER program (CIrculation THERmohaline) between January and March 1993. Two zonal sections at 4°30 S and 7°30N (the A7 and A6 WOCE sections) and two meridional sections at 35°W and 3°50 W were sampled for CFMs between the African and South American continents. The results reported here deal primarily with the North Atlantic Deep Water. The CITHER 1 sections were made just 10 years after the first CFMs snapshot of the tropical Atlantic ocean obtained during the Transient Tracers in the Ocean Program.

The detection limit was approximately 0.0025 pmol.kg^{-1} for both F-11 and F-12. This is sufficient to allow the determination of "apparent" ages and dilution factors for the *freon*-enriched tongues of the Upper and Lower North Atlantic Deep Water (UNADW centered around 1600 m and LNADW centered around 3800 m).

Both zonal sections clearly show the propagation of UNADW into the eastern basin. The eastern meridional section at 3°50W shows the CFM cores extending from 4°S to 3°N with a maximum around 2°S. From the equatorial CFM ratios in the eastern basin, we estimate an eastward velocity close to 2 cm/s.

The CFM distributions at the levels of the UNADW and LNADW show a large variability, probably linked to northern and southern deep recirculation gyres. In both sections, CFM enriched cells are clearly the result of reversed currents.

The net decrease of CFM in the LNADW between 7°30N and 4°30S is partly the result of the bifurcation of the deep flow north and at the equator. This is confirmed by data taken in November 1992 in the region of the Equatorial Romanche Fracture Zone by the ROMANCHE 2 cruise.

The influence of Antarctic Bottom Water is noticeable along the South American continent in the southern section. There is no evidence, through CFM data alone, for a northward flow of this "young" bottom water mass, which is probably blocked by the topography near the sampled areas.

Introduction

The 1983 TTO data set, (Weiss et al. 1985), is often used as a benchmark for F-11 studies of the Atlantic. The data shows the flow of the Deep Western Boundary Current (DWBC) from 50°N to 10°S and indicates a southward and eastward splitting of the flow near the equator at the level of the "young" Upper North Atlantic Deep Water (UNADW). Ten years after TTO, one objective of the CITHER 1 cruise was to follow the evolution of the tracer concentration in the tropical region, in particular concentrating on the trans-equatorial and equatorial transport of the NADW.

After 1985, several studies concerning NADW transports and CFMs distributions in the tropical Atlantic ocean have been reported. They principally concern tracers description into the DWBC (Fine and Molinari 1988; Pickart et al. 1989; Pickart 1992; Molinari et al. 1992; Pickart and Smethie 1993; Smethie 1993; Rhein 1994; Rhein et al. 1995). Centered around 1600-1700 m, the enriched

From WEFER G, BERGER WH, SIEDLER G, WEBB DJ (eds), 1996, *The South Atlantic: Present and Past Circulation.* Springer-Verlag Berlin Heidelberg, pp 273-288

CFM core, classically corresponding to the Upper NADW (UNADW), is more precisely identified as the recently ventilated water mass originating from convection in the southern Labrador sea. At a denser level, the Lower NADW (LNADW), centered around 3800 m, originates from the Denmark Strait overflow. Mc Cartney (1993) discusses the previous considerations concerning the question of the DWBC bifurcation at the equator and the zonal advection velocities inferred from tracer distributions. Recirculation processes are assumed to be responsible, in part, for the tongue shape of the CFM distributions and for the underestimation of the DWBC flow velocity along the western boundary of the tropical Atlantic.

During the CITHER 1 cruise, in January-March 1993, four sections were sampled at 7°30N, at 4°30S (A6 and A7 sections of the World Ocean Circulation Experiment WOCE), and at 35°W and at 3°50 W (Fig. 1).

This paper reports informations inferred from CFM data only. Hydrological and other tracers (oxygen, nutrients) data are reported in the CITHER 1 Reports (Le Groupe CITHER-1 1994 a, b, c).

The analytical procedure is presented in section 2. In section 3, we describe and discuss CITHER 1 CFM distributions in order to infer a schematic circulation pattern of the NADW, principally concerning recirculation and eastward bifurcation near the equator. In section 4, informations relative to the use of the "apparent age" evaluated from the CFM ratio method are presented and discussed, and the CITHER1 F-11 sections are compared to the TTO section (Weiss et al. 1985).

Methods

Seawater samples were obtained using the IFREMER rosette equipped with 32 8l-bottles. 188 stations were sampled for F-12 and F-11, at 32 levels regularly spaced from the surface to the bottom, with a separation of less than 60 n.m.

The technique used for CFM measurements on board was the extraction-trapping method coupled to gas chromatography, with electron capture detection, described by Bullister and Weiss (1988). The data reported here are based on the Scripps Institution of Oceanography (SIO) 1986 calibration scale using a primary standard provided by SIO. The accuracy of the secondary standard used on board is 0.9% for F-12 and 0.8% for F-11.

Atmospheric measurements were performed daily all along the cruise. A weak latitudinal gradient was observed between 7°30N and 4°30S (around 0.45 ppt/°lat for F-12 and 0.3 ppt/°lat for F-11). No noticeable zonal gradient was observed. The mean atmospheric mixing ratios are 513.8 ± 4.2 ppt for F-12 and 276.0 ± 3.2 ppt for F-11 at 7°30N and 508.3 ± 4.9 ppt for F-12 and 272.4 ± 3.1 ppt for F-11 at 4°30S.

The mean deviation of the measured surface concentrations to the theoretical solubility values (Warner and Weiss 1985) was found to be close to 1% for both F-12 and F-11. This value, near the solubility equilibrium, is expected in the tropical area in the northern winter season. The values relative to the stations close to the African continent have been excluded from this global mean. This is because under-saturation, sometimes exceeding -15%, were found near the coast due to coastal upwelling.

The results of five test-stations for bottle "blanks" determinations (32 bottles sampled at one same deep level, assumed to be *freon*-free) were used to determine the detection limit of the method. The precision of the method for deep samples is given by the standard deviation of the mean bottle contamination level. It is around 0.0025 $pmol.kg^{-1}$ for F-12 and for F-11. The mean bottle contamination levels measured by this method vary in the ranges 0.001-0.008 $pmol.kg^{-1}$ for F-12 and 0.007-0.013 $pmol.kg^{-1}$ for F-11. A net decrease of the contamination level occurred during the cruise as the bottles became cleaner. The final CFMs concentrations are corrected for this contamination using a "blank" level interpolated between the test-stations. The reproducibility has been checked at least once at each station by sampling two bottles at the same depth. In addition, some stations were reoccupied during the cruise; the deviation between the profiles of stations 119-156 (15 days apart) at 35°W, 7°30S being less than 0.5%.

For the deep levels, direct velocity measurements (Pegasus profiles have been performed on the 35°W section) or indirect geostrophic calculations relative to the zonal sections are not presently available.

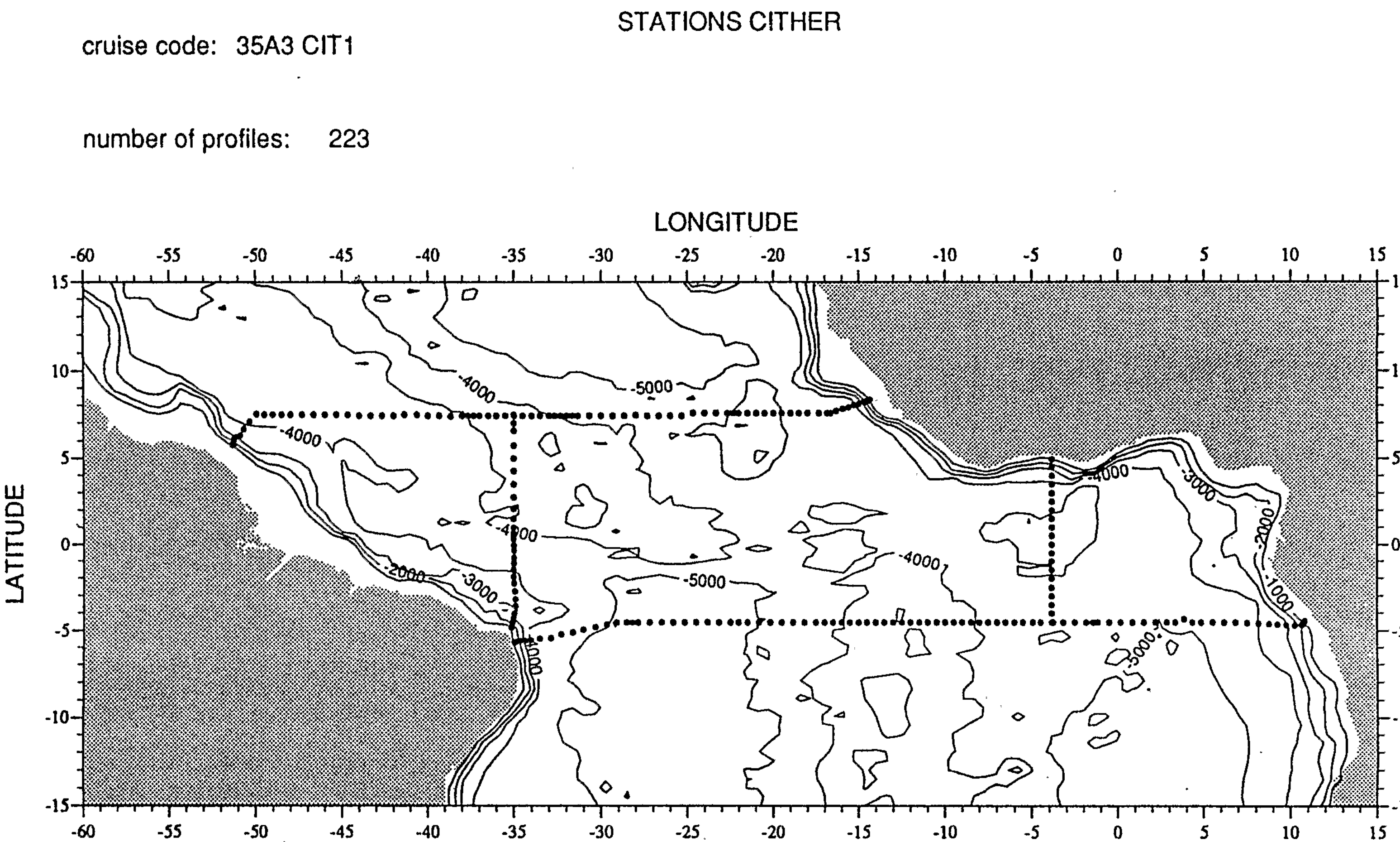

Fig. 1. Stations location of the CITHER 1 cruise in January-March 1993 surimposed on a bathymetric chart showing isobaths at each 1000 m interval.

F-11 distributions

Figs. 2 a, b, c and d show the F-11 distribution along the 7°30 N, 4° 30 S, 35°W and 3°50 W sections. F-12 distributions are very similar (Andrié and Ternon 1994). The different features observed, often associated with the movement of different water masses, are discussed in the following sections.

freon-free water masses

A *freon*-free water mass is a permanent feature of the Atlantic ocean around the 1000m depth level. This level was described by Kawase and Sarmiento (1986) as poorly ventilated (with a low oxygen concentration) and rich in nutrients. The absence of F-11 at this depth, in the northern section as well as in the southern section, indicates that the water mass corresponds to the Upper Circumpolar Water (UCPW) (Fine and Molinari 1988; Reid 1994) rather than to the Antarctic Intermediate Water (AAIW) as suggested by Friedrichs (1992) and Tsuchiya et al. (1994). The absence of F-11 signal (and oxygen signal) excludes the possibility of an input of a younger water mass such as AAIW at this level.

The layer between 2200 and 3800 m is principally *freon*-free (except at the western boundary) and corresponds to the Middle NADW (MNADW). This water mass includes the oxygen-rich Labrador Sea Water (LSW) and the old NADW originating from the Gibbs Fracture Zone (Rhein et al. 1995; Reid 1994). Circumpolar Water (CPW) coming from a southern origin is also found in this depth range (Reid 1994; Tsuchiya et al. 1994; Talley and Johnson 1994; Rhein et al. 1995). Due to the diversity of these possible origins, it is not obvious to determine the origin of some small CFM enriched structures which sporadically appear in this depth range.

Below 4000m depth and above the level of the Antarctic Bottom Water (AABW), the CFM-free waters correspond to the Lower Circumpolar Water (LCPW) (Tsuchiya et al. 1994).

CFM-enriched tongues

Upper NADW

The upper tongue corresponds to shallow UNADW (or suNADW after Rhein et al. 1995). This water mass originates in the southern Labrador Sea Water (Pickart et al. 1989; Smethie 1993) and is found in the depth range 1600-1700 m in the tropical Atlantic. The eastward extension of the 0.01 pmol/kg isoline reaches 27°W at 7°30 N (Fig. 2a) and 0°W at 4°30 S (Fig. 2b). On the western boundary, the maximum intensity of the core exceeds 0.2 pmol/kg in the north while it is half this value at 4°30 S.

The 7°30N F-11 vertical section (Fig. 2a) is very similar to the one obtained by Molinari et al. (1992) during February 1989 along a 200 km zonal transect at 14°30 N. The upper core extends across the western basin and reaches 27°W in the eastern basin. A similar extension into the eastern basin is also observed in the 3°50W section (Fig. 2d). This is the first time that an F-11 signal, exceeding 0.04 pmol/kg at 2°S, has been reported east of 18°W (Doney and Bullister 1992) and provides evidence for the equatorial bifurcation at the flow. On the southern 4°30S section (Fig. 2b) the upper core also crosses the Mid Atlantic Ridge.

At 35°W, as observed in October 1990 and June 1991 by Rhein et al. (1995) in the DWBC, the equatorial F-11 maximum core is split into one maximum centered around 1°S, and a second one north of 0°30N (Figure 2c). In addition our data clearly show a northward extension of the F-11 core as far as 6°N (Fig. 2c) which could be due to the input of an eastward flow coming at the latitude of the Ceara rise.

McCartney (1993) does not attribute the offshore displacement of the core to a shift of the dominant flow path but, partly, to the erosion processes occuring between the overlying UCPW (just below the AAIW level) and the UNADW flowing in opposite directions. The isolation of the northward core by a relative F-11 minimum around 3°N seems to be due to recirculation process discussed below.

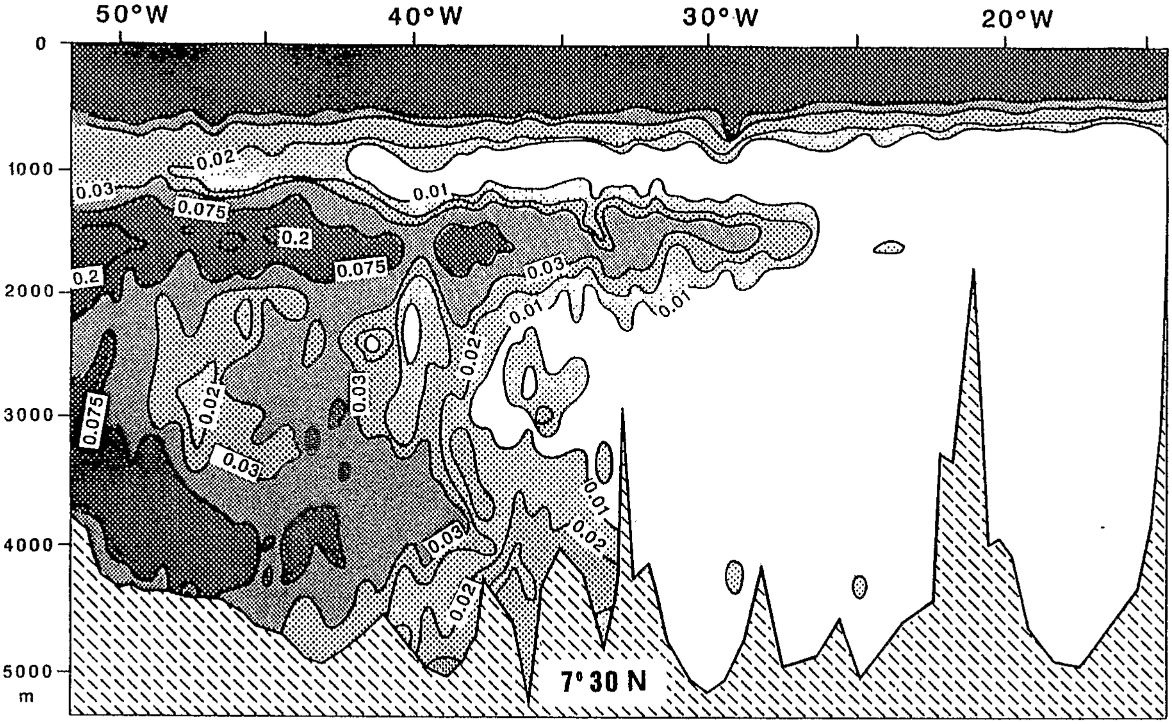

Fig. 2. F11 distributions during CITHER1 a) northern F11 section (WOCE A6) at 7°30N (contours in pmol/kg)

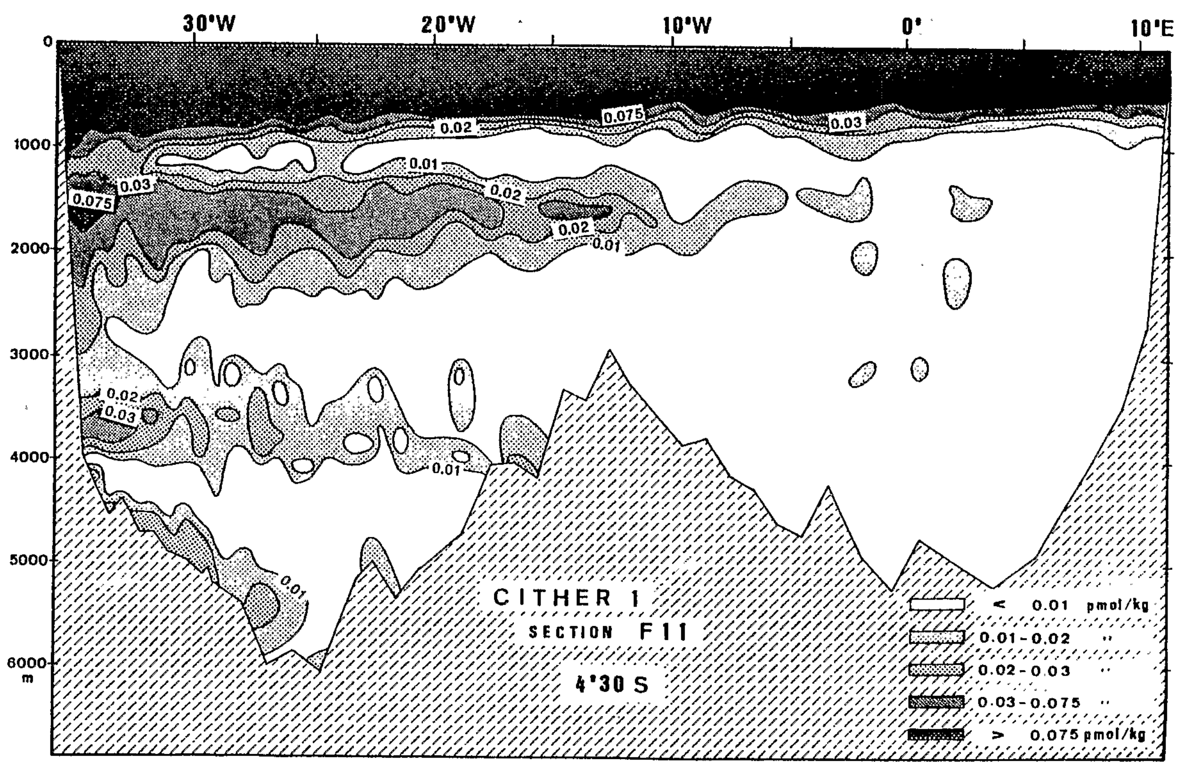

b) southern F11 section (WOCE A7) at 4°30S (contours in pmol/kg)

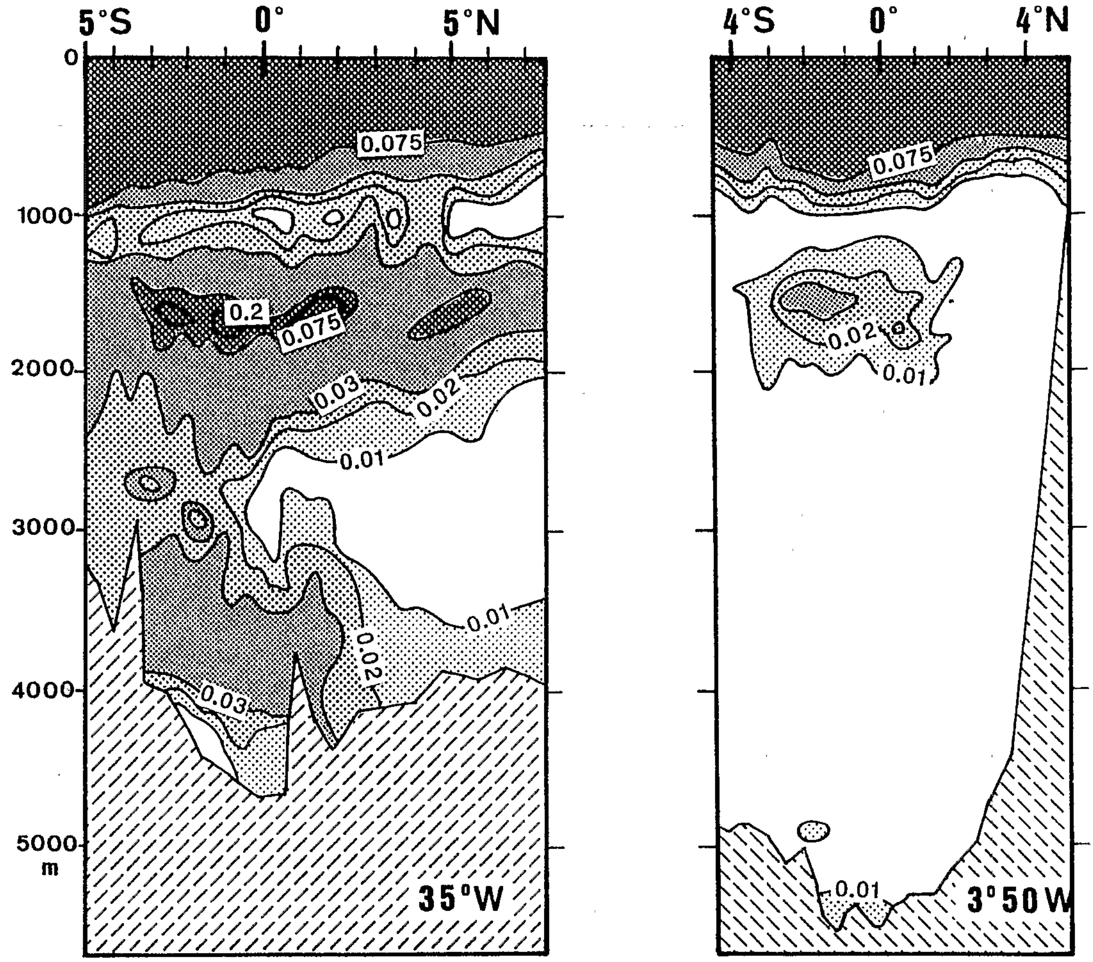

Fig. 2. F11 distributions during CITHER 1

c) meridional western F11 section at 35°W (contours in pmol/kg)
d) meridional eastern F11 section at 3°50 W (contours in pmol/kg)

Previous observations upstream in the DWBC at 14°N (Molinari et al. 1992) have shown that the F-11 cores coincide with southward velocity cores with, sometimes, some patchiness in the tracer structures. South of the equator, the F-11 cores agree with the F-11 distributions and permanent eastward transports described by Rhein et al. (1995) for the 1990-1992 period.

Lower NADW

The lower tongue centered around 4000m depth corresponds to the LNADW overflow water (ov-NADW after Rhein et al.1995), originating from the Denmark Strait (Pickart et al. 1989; Smethie 1993). At 7°30N (Fig. 2a), the extension of the 0.02 pmol/kg isoline observed as far as 30°W for the upper tongue is less pronounced (40°W) for the lower tongue.

At 4°30S (Fig. 2b), the F-11 concentrations in the lower core are considerably reduced compared to the northern section (Fig. 2a). This is probably the result of two successive blockings of the LNADW. The first, just north of the Ceara rise at 5° N, diverts the core offshore (see the 4000 m isobath on Fig. 1). The second, near the equator, is due to the equatorial channel. This is the valley (deeper than 4000 m) located between the southern wall of the Mid Atlantic Ridge, near the equator, and the eastward extension of the continental rise (Parnaiba Ridge), near 3°S, (Speer and McCartney 1991; McCartney and Curry 1993).

On the western boundary, the F-11 content maximum in the lower core reaches 0.1 pmol/kg at 7°30N while it is only 0.04 pmol/kg at 4°30S. At 35°W (Fig. 2c), the F-11 core corresponds to the permanent eastward flow centered around 1°40 S as already mentioned by Rhein et al. (1995). The F-11 maximum is principally concentrated in the equatorial channel between the Parnaiba Ridge at 2°S and the equator.

The implications concerning the bifurcation of the flow along the equator and the deep recirculation gyres are discussed later in the paper.

The results also shed some light on a question proposed by Bennekom (this issue) concerning the origin of the Angola basin deep waters. He argues, from silica data, that the bottom water observed in the Angola basin north of 30°S is predominantly NADW coming from Chain and Romanche fractures. Wallace et al.(1994) report in the deep Angola basin, at 19°S, significant CCl_4 concentrations but no-trace of F-11 on the eastern side of the Mid Atlantic Ridge : the CCl_4 signal is assumed to be derived from waters coming from the North (through the Romanche fracture zone) or from the South (through or over the Walvis ridge). The low F-11 concentrations observed during CITHER 1 on the southern section (Fig. 2b) and on the equator along the 3°50 W section (Fig. 2d) and at the exit of the Romanche Fracture Zone during the ROMANCHE 2 cruise (Messias 1994) do not indicate a southward flow of NADW along the eastern side of the Mid Atlantic Ridge. The weakness of the F-11 signal is not incompatible with a CCl_4 signal at 19°S due to the shorter F-11 story in the atmosphere (injected since 1945) compared to the CCl_4 one (injected since 1920). The question of the origin of the Angola basin deep waters is still open.

Antarctic Bottom Water

The variability in F-11 found at the AABW level is as high as that observed at upper levels. The southern, 4°30S, section (Fig. 2b) exhibits a F-11 enriched core, lying on the bottom below 4500 m, corresponding to the AABW. This core is most noticeable on the western side of the Brasil basin, near the South American continent. As mentioned by Rhein et al. (1995), this water mass is CFM enriched by mixing with the underlying more recently ventilated Weddell Sea Water component. Tushiya et al. (1994) describe more precisely the distinction between the AABW (from LCPW origin) and the WSDW.

On the 35°W section (Fig. 2c), the results confirm the Rhein et al. data of 1990-1992, the AABW signal does not seem to cross the equator, being blocked by the topography. McCartney and Curry (1993) propose two features that probably restrict the northward flow of AABW. The first is the sill (4500 m) at the entrance of the equatorial channel. The second is the Ceara rise, which acts as a barrier for waters deeper than 4500 m between 1°N and 4°N. At 35°W, there is a small F-11 signal in the northern side of the equatorial channel near the equator suggesting an AABW westward flux near the bottom (around 4600m depth). The weakness of the F-11 signal near the equator can be associated with the absence of a F-11 signal in the depth range of the AABW at the entrances of the Romanche and Chain fractures as mentioned by Messias (1994). The bottom water near and north of the equator has a predominant LCPW influence.

Bifurcation of the NADW flow at the equator

Fig. 3 shows the horizontal distribution of the 0.015 pmol/kg and 0.05 pmol/kg isolines inside the tropical area at the UNADW level (1600 m), obtained by interpolating between the four sections reported above. Superimposed are the F-11 isolines corresponding to the 1983 TTO data set. Compared to the TTO distributions, the new data emphasizes the reality of the UNADW core bifurcation along the equator.

The F-11 data at the 3°50W section in the eastern basin give evidence for a bifurcation of the UNADW flow near the equator (Fig. 2 d). However, the core maximum is somewhat shifted south of the equator (around 2°-3° S). The bifurcation could be induced by the rise (around 2000 m depth) of the Parnaiba ridge near 3°S (Fig. 2 c). In addition, we observe on the 35°W section (Fig. 2c) a secondary F-11 enriched core centered around 5°N which can be due to an input of an eastward flow coming along the Ceara rise.

The eastward bifurcation just south of the equator is in agreement with Tsuchiya et al. (1992, 1994) who report through two different salinity sections at 20°W and 25°W an eastward core centered around 2°S.

The circulation pattern inferred from our data at the UNADW level (Fig. 4) shows the eastward bifurcation of the DWBC flow near the equator and reversed flows both sides of the equator. It is similar to the general circulation scheme proposed by Richardson and Schmitz (1993) from drifting floats, on the 1800 m level (Fig. 5).

There is also evidence for an eastward bifurcation of the LNADW core, particularly through the strong north-south latitudinal gradient observed in F-11 concentrations (Fig. 2 c). As discussed above, this bifurcation is principally induced by bathymetric effects of the Ceara rise and then by the equatorial channel. The location of the F-11 core corresponds to the mean flow described by Rhein et al. (1995) i.e. guided by the topography and concentrated on the southern side of the equatorial channel. There is no F-11 enrichment north of 2°N on the 35°W meridional section (Fig. 2c). This means that the LNADW flow does not continue

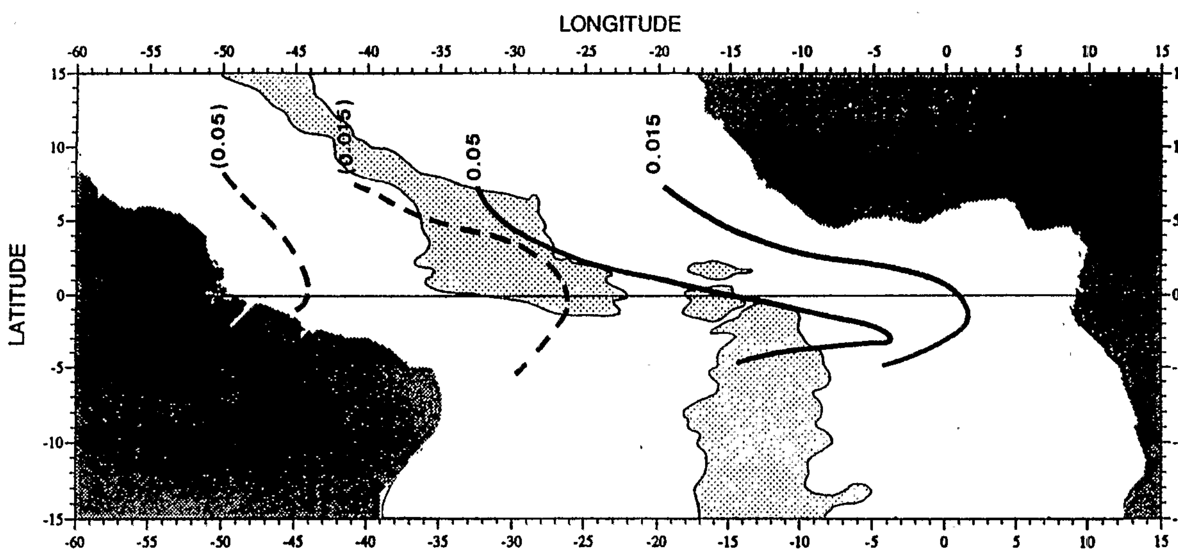

Fig. 3. TTO-CITHER 1 F11 distributions comparison (0.015 and 0.05 pmol/kg isolines). The 0.015 and 0.05 isolines relative to the 1983 data set (broken lines) are indicated in parenthesis. Surimposed is the 4000m depth isobath at the location of the Mid Atlantic Ridge.

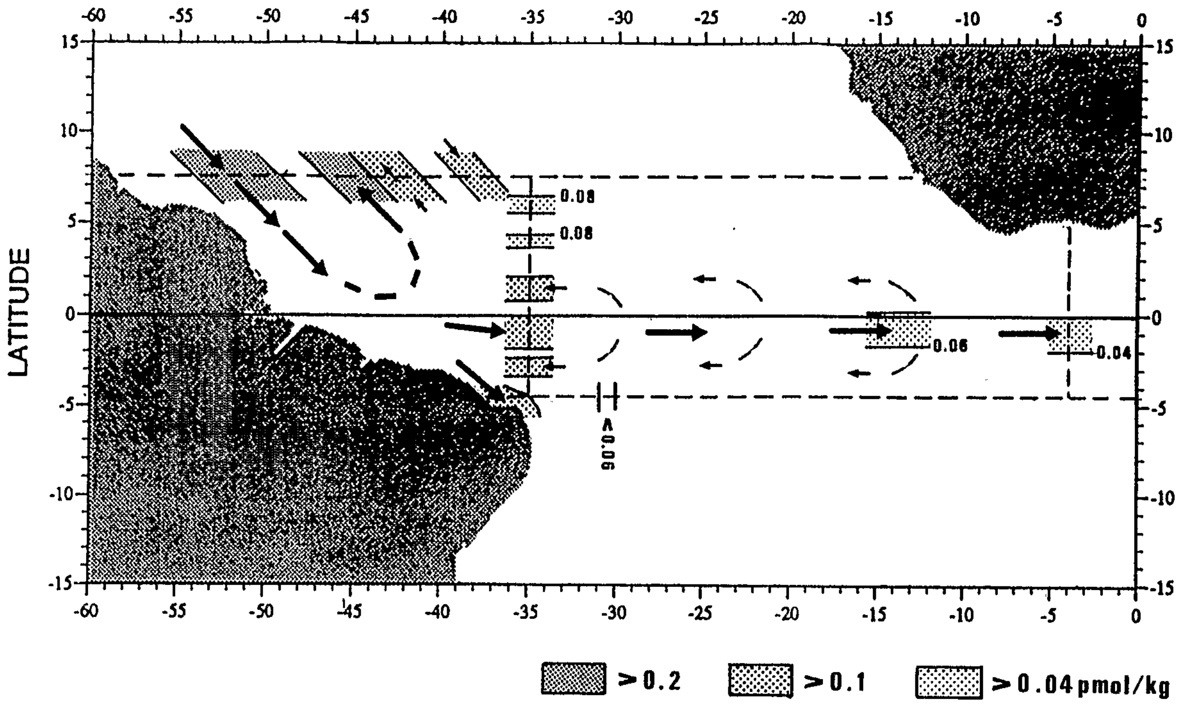

Fig. 4. Schematic circulation pattern inferred from the F-11 distributions at 1600 m depth.

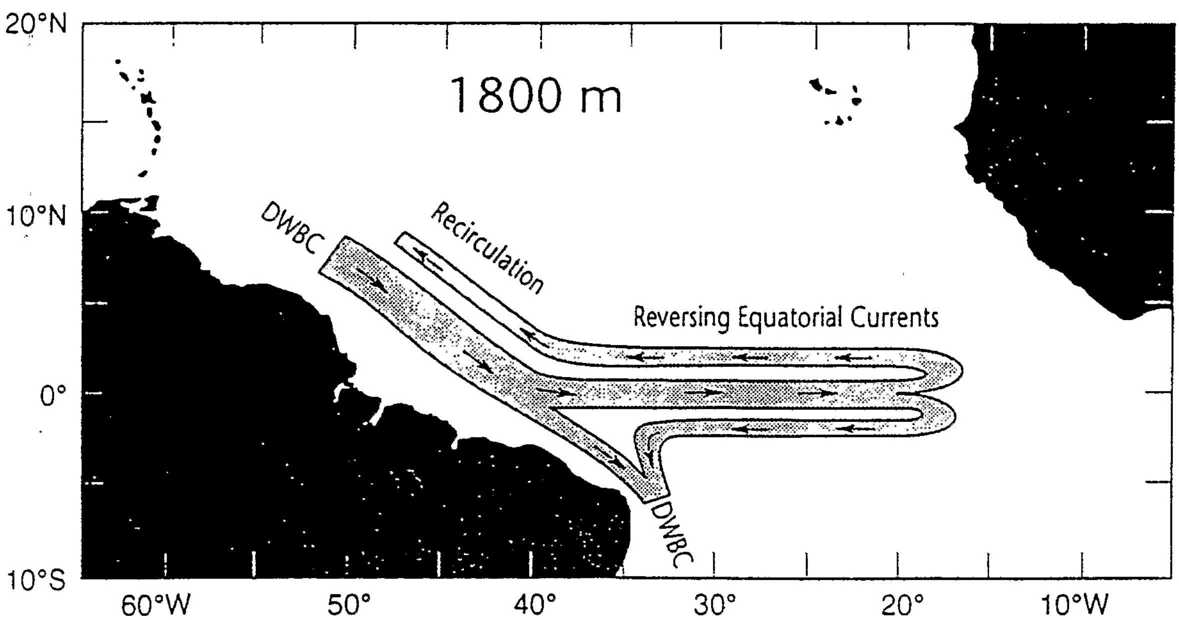

Fig. 5. Recirculation scheme proposed by Richardson and Schmitz (1993) at 1800 m.

eastward (east of 40°W) but turns southward just after the Ceara rise blocking near 5°N.

The equatorward flow is partially blocked by the Mid AtlanticRidge (Fig. 2b) but enters into the eastern basin through the Romanche Fracture Zone near the equator. The LNADW has been clearly identified into the Romanche Fracture through F-11 and F-12 data (Messias 1994). After the sills, the LNADW core deepens and mixes with CFM-free surrounding waters. At 3°50 W (Fig. 2d), a F-11 signal is observed for depth greater than 4800 m, probably as the result of the "cascading" and the spreading of the LNADW coming through the Romanche Fracture Zone after the sills.

Deep recirculation gyres

Recently, several authors (Weiss et al. 1989; Molinari et al. 1992; McCartney 1993; Friedrichs et al. 1994; Rhein et al. 1995) have suggested that the assumption of a conservative flow in the DWBC responsible for the southward advection of the nordic ventilated waters was too simplistic to explain the shape of the tracer distributions : effects of recirculation gyres have been discussed. The most striking feature in the CITHER 1 F-11 distributions, clearly delimited due to the fine space and depth resolution of the sampling, is the extremely heterogeneous structure of the deep F-11 distributions. The F-12 distribution (Andrié and Ternon 1994) indicate a similar heterogeneity of the water masses.

McCartney (1993) has described two important deep recirculation gyres : the Guiana cyclonic abyssal gyre (in the Demerara plain), centered north of the equator and extending down to 1°S and the Brazil anticyclonic abyssal gyre (centered near 11°S). The existence of a northern abyssal recirculation is also demonstrated in the numerical model of Kawase (1993). This indicates that AABW has a northern limit at 25°N in the east of the Guiana basin. Other circulation patterns have been reported by Friedrichs et al. (1993, 1994) for the MNADW and the LNADW. Durrieu de Madron and Weatherly (1994) give circulations patterns for NADW and AABW south of the equator and an eventual connection between northern and southern recirculation cells; they describe the interior upwelling occurring between the AABW and the NADW.

Fig. 4 shows the main circulation features inferred from the CITHER 1 F-11 data set at the UNADW level. The locations of the F-11 maxima suggest the existence of a recirculation cell north of the equator, responsible for F-11 concentrations as high as 0.2 pmol/kg at 7°30 N in the DWBC and, eastward, near 45°W (Figs. 2a and 4). This second F-11 maximum indicates the possible presence of the eastern limb of a recirculation gyre which is responsible for advecting the tracer northward. This feature does not appear in the Richardson and Schmitz pattern (Fig. 5). The F-11 maximum observed at 1°N on the 35°W section and the discontinuity (> 0,06 pmol/kg minimum at 4°30S around 31°W, Fig. 4) could be intrepreted as the effect of the continuity of the eastern limb : but the higher F-11 concentration in the northern recirculated limb (> 0.2 pmol/kg near 45°W) than in the south (0.1 pmol/kg), suggests that the northward turning of the recirculation gyre must occur north of the equator. The wide extension of the F-11 core (as far as 49°W, Figs. 2b and 4) is partly due to the superimposed inputs of the flow of the DWBC itself and of the western limb of the cyclonic Guiana recirculation gyre.

At 7°30 N, the location of the western F-11 relative minimum (49°- 52 °W, Fig. 4) is about 400-500 km away from the DWBC core and corresponds to the area located between both branches of the recirculation pattern: the flow of the water mass here is weaker and associated to a weaker tracer input. Farther east, around 39°- 42°W, there is a F-11 mininum which seems to correspond to the southward flow along the western side of the Mid Atlantic Ridge, as mentioned by Friedrichs and Hall, 1993. The discontinuities in the upper core may be due to disruptions in the zonal advection flow or to the transient tracer input during the last 20 years (Weisse et al. 1994).

On the 35°W section (Fig. 2c and 4) we observe, near the American coast (around 3°S), the F-11 maximum corresponding to the DWBC core. Farther north (around 2°S), another F-11 enriched core, corresponds to the eastward bifurcation of the mean flow. In between, a third F-11 core could be explained by a reverse westward recirculated flow south of the equator. Another reverse flow near the equator seems evident around 1°-2°N (Fig. 2c and 4). Features like these have already been identified in floats trajectories at 1800 m (Richardson and Schmitz 1993) but not in exactly the same area (Fig. 5). The intensity and the location of the direct and reverse equatorward flows could be variable.

The major circulation features which affect the deep F-11 distributions in the LNADW core are, as mentioned above, the result of topographic effects. The LNADW turns eastward near 5°N due to the blocking effect of the Ceara rise, then flows southward after the Ceara rise and is deflected eastward into the equatorial channel to cross the Mid Atlantic Ridge through the Romanche Fracture Zone.

Recirculation processes due to the Guiana cyclonic gyre are also noticeable at the LNADW level (Figs. 2a and 2b). This shows two separated cores on both northern and southern sections. At 7°30 N the eastern limb is located between 42°W and 44°W, somewhat further offshore than for the UNADW level. In the south at 4°30 S (Fig. 2b), the western core, located around 3800 m, lies adjacent to the coast. A second core is located between 26°W and 28°W, around 750 km offshore from the western limb. The recirculation effect is also noticeable down to the level of the AABW, where two F-11 cores appear at the same longitudes as the LNADW cores.

In conclusion, the Guiana abyssal recirculation gyre is well identified through the whole water column between the bottom and the UNADW level. In addition at the depth of the MNADW, on both northern and southern sections, the *freon*-free water mass (F-11 concentration less than 0.04 pmol/kg), indicate two F-11-enriched "chimney-like" structures, which may identify the center of the recirculation gyre.

Apparent ages and dilution factors

CFMs are often used as tools to determine the "age" of water masses (Bullister 1989; Fine et al. 1988). The knowledge of the time evolution of F-11 and F-12 since the time of their injection into the atmosphere allows one to evaluate the "age" of previously ventilated water masses i.e the elapsed time since the water parcel left the atmosphere-ocean interface. This method is only valid for the period between 1945 and 1975, since the beginning of the CFMs injection into the atmosphere to the limitation of their production.

Time evolutions of the F-11 content and the corresponding F-11/F-12 ratio in the UNADW source waters are shown in Fig. 6. These theoretical values correspond to the solubility equilibrium values at the temperature and salinity characteristic of the UNADW. They are calculated from the solubility functions of F-11 and F-12 reported by Warner and Weiss (1985) and the atmospheric mixing ratios time evolution (Weiss, personal communication) for the northern hemisphere.

Assuming a CFM-enriched water mass flowing into a *freon*-free environment, the F-11/F-12 ratio of the water parcel is conservative along the flow. So, its measurement allows to determine the "apparent age" of the water mass. The knowledge of the apparent "age" (F11/F12 curve from Fig. 6) allows determination of the theoretical F-11 concentration (F-11°) that the water mass should have at the time of the water mass formation (from Fig. 6): the ratio F-11°/F-11 (F-11 represents the F-11 concentration at the time of the measurement) allows to determine the "apparent" dilution factor.

Recent work on transient tracer distributions, particularly in the Deep Western Boundary Current, have shown difficulties inherent to turbulent mixing processes, occuring between the mean flow and surrounding water, and responsible for a bias in apparent ages or velocities determination (Pickart 1992; Smethie 1993; McCartney 1993; Rhein 1994). In this paper we deal primarily with the CFM eastward penetration into a completely *freon*-free environment. Under these conditions, apparent ages and dilution factors can be considered valid without much correction for mixing. An apparent zonal velocity along the equator can thus be deduced. This evaluation has to be considered as a mean "integrated" value as it takes into account the whole water mass history from the CFM source area.

Due to the uncertainties in the following effects, no corrections have been made for the CFM undersaturations in the formation areas (Wallace and Lazier 1988; Rhein 1991), for the residence times in the sources reservoirs (Pickart et al. 1989 ; Rhein

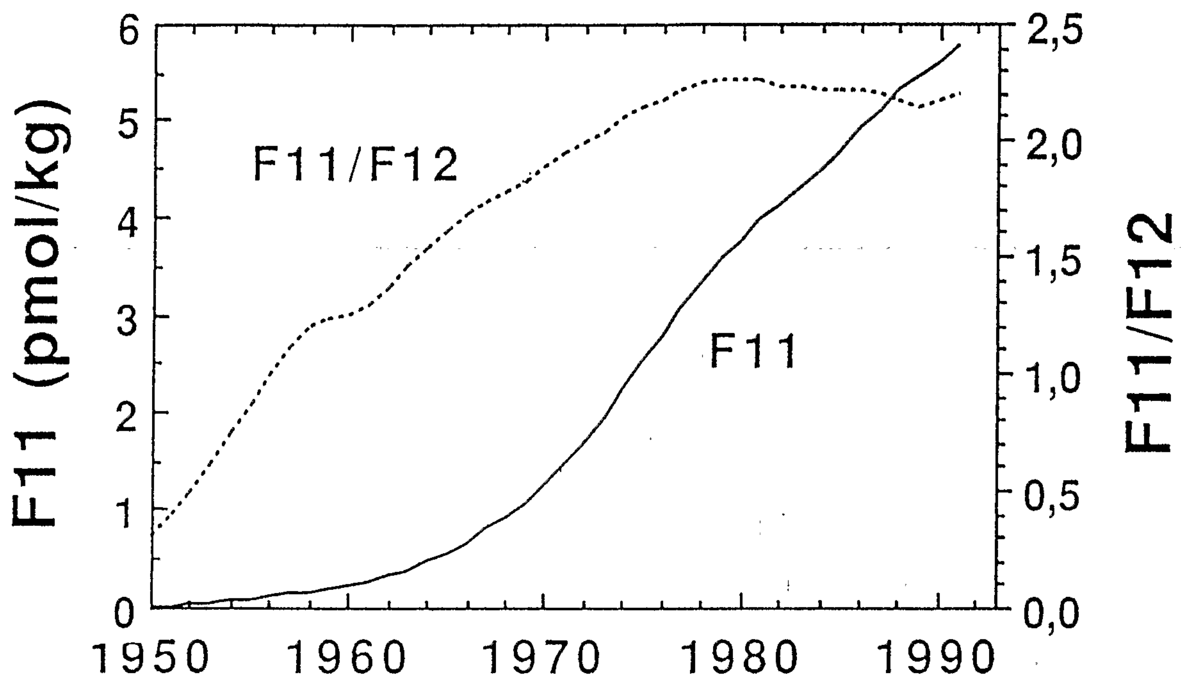

Fig. 6. Evolution with time of the theoretical oceanic F11 concentration evaluated from the time history of the atmospheric F11 concentrations (Weiss personal communication). The temperature and salinity of the UNADW are used in the solubility function of Warner and Weiss (1985).

1991) nor for self-mixing (Pickart et al. 1989; Rhein 1994). Consequently, the reported evaluations have to be considered as minimal values.

Table 1 gives the upper core mean characteristics between the DWBC and the 3°50W section, the F-11 content at the core maximum, the associated F-11/F-12 ratio, the apparent velocity and the apparent dilution factor.

As mentioned above, the use of F-11/F-12 ratios in apparent velocity and dilution factor calculations gives considerably biased estimations when self-mixing of an advected water mass occurs (apparent velocity is underestimated): we have shown in section three that it is typically the case for the NADW inside the DWBC. Consequently, the results relative to apparent age, apparent velocity and dilution factor reported in Table 1 for 50°W and 35°W are presented only for comparison with 3°50 W estimations but must not be considered as representative values. The speed flow deduced by the F-11/F-12 age method in the DWBC is well below the values obtained by direct observations : Johns et al. (1993) give a mean value inferred from a current meter mooring at 8°N, 52°W, in the DWBC, of about 28 cm/s (annual mean) below 4000 m. Schött et al. (1993) describe a highly variable deep currrent from moored stations at 44°W, near the equator, with an annual mean speed around 30 cm/s. Colin and Bourlès (1994) report Pegasus velocity measurements greater than 50 cm/s in the area 5°N-10°N within the upper core of the DWBC. The same order of magnitude is inferred from SOFAR floats trajectories (velocities higher than 50 cm/s at 1800 m) in the DWBC. On the opposite, we consider that the results concerning the 3°50 W section are significant because the calculations are made near the eastern edge of the CFM tongue, for a water mass assumed to have been, from its northern source to the eastern tropical Atlantic, in a completely *freon*-free environment. They agree well with the few direct estimates inferred from current meters measurements (Ponte et al. 1990) or floats (Richardson and Schmitz 1993) which, despite a great seasonal and interannual variability, lead to

Table 1: Apparent ages and dilution factors inferred from the F11/F12 method for the UNADW.

eastward from the DWBC	7°30N-50°W (DWBC)	35°W	3°50 W
F11 max	0,26 pmol/kg	0,11 pmol/kg	0,05 pmol/kg
F11/F12	2,1 ± 0,05	1,72 ± 0,14	1,7 ± 0,4
apparent age	1974 ±1 19 years	1968 ± 3 25 years	1967 ± 6 26 years
apparent velocity	1,6 cm/s	1,5 cm/s	1,9 cm/s
dilution factor	8 ± 0,5	12 ± 5	60 ±30

a mean eastward value in relative agreement with our estimated value. The indirect approaches reported by Kawase et al.(1992) or Böning and Schott (1993) agree with the existence of a mean, weak, eastward current along the equator of the same order of magnitude as our estimate. However, taking into account the previously mentioned limitations of the F11/F12 aging method, our age and velocity estimations must be considered as tentative.

Comparison between 35°W and 3°50 W (Table 1) cannot indicate wether the increase of the dilution factor eastward is true, or is due to the underestimation linked to the F-11/F-12 method in areas where mixing and/or recirculation occur.

TTO data and CITHER 1 results comparison :

Previously reported comparisons with the first F-11 1983 TTO data set (Weiss et al. 1985) have been made by Weiss et al. (1989) and Molinari et al. (1992). We derive, by a similar approach, completely independent from the F-11/F-12 ratio method, a second estimate of the zonal advection velocity.

For comparison, the CITHER 1 1993 F-11 distribution obtained by interpolation between our 4 sections are superposed to the TTO 1983's one (Fig. 3). Despite the very coarse resolution of this scheme, it allows us to observe the eastward progression of the transient tracers between 1983 and 1993. The southward shift of the UNADW core is well noticeable on the 0.05 pmol/kg contour.

We have choosen to follow the eastward displacement of the 0.05 pmol/kg instead of the 0.015 pmol/kg contour. The latter is very close to the detection limits of the analytical systems and the comparison between 1983 and 1993 data could be biased by a possible difference between both experiments. The choice of the 0.05 pmol/kg contour, still a low-concentration level not really affected by dilution with non-*freon*-free waters, seems more reasonable.

In these conditions, we deduce a mean zonal velocity of 1.4 cm/s inferred from the 4440 kms eastward displacement (from 43°50 W to 3°50 W) of the 0.05 pmol/kg isoline during 10 years. This evaluation yields a value close to the values obtained by the F-11/F-12 ratio method in the east (1,9 cm/s at 3°50 W, Table 1). The small discrepancy can be due to the fact that the second method, considering the F-11 concentrations alone, does not take into account the dilution effect and, so, can be responsible for an underestimation of the advection velocity. Anyway, the deviation between both evaluations can, in part, be explained by the detection limits of the two methods.

Conclusion

The CITHER 1 CFM data set contains significant new information on the deep circulation of the tropical Atlantic. This is particularly true for the North Atlantic Deep Water.

The data set provides evidence for an eastward bifurcation of the DWBC and a zonal advection of the UNADW along the equator. This eastward flow can be followed as far as 4°W. It is shifted southward around 2°30 S and opposing currents are identified north and south the main core. For the LNADW, the CFM content decrease between the 7°30N and the 4°30S sections. This is principally a result of the topography. An initial eastward bifurcation occurs north of the Ceara rise near 5°N, after which the DWBC seems to flow southward again. Later, an eastward bifurcation of the LNADW flow is identified in the south of the equatorial channel near 2°S.

A new observation coming from the CITHER 1 data is the great spatial variability in the F-11 distribution due to recirculation processes and interior upwelling. The existence of the abyssal Guiana cyclonic gyre (McCartney 1993) is confirmed. It shows up particularly well on the UNADW and LNADW levels through the presence of two distinct F-11 cores at the locations of the western and eastern limbs of the gyre. The southern limit of this gyre is found to occur north of the equator.

The CFMs allow determination of the "apparent age" of the NADW. From the F11/F12 ratio method we determine an eastward "apparent velocity" close to 2 cm/s. An evaluation of similar magnitude is obtained when comparing the 1983 TTO F-11 data with CITHER 1 ones taken ten years later. The discrepancy observed between velocities inferred from the F11/F12 method and direct measurements is due to the particular approach concerning the use of transient tracers such as CFMs: the F-11/F-12 method leads to a mean velocity of the flow, from the source region to the studied area, which includes the effects of turbulent mixing and recirculation. From a general-circulation point of view, the tracer approach is more realistic than a direct measurement of the advection velocity (Doney and Jenkins 1994).

A study including examination of hydrological, nutrients data and geostrophic transports is in progress (Andrié et al. in prep.). It should greatly improve our first conclusions on the deep circulation in the tropical Atlantic derived from F-11 and F-12 measurements alone.

Acknowledgements

The author specially thanks C. Oudot, responsible for the CITHER 1 program and A. Morlière and C. Colin, chief scientists of the two legs. The captains and all the crew of the R.V. Atalante have made possible the *freon* measurements in very good conditions on board. The help of M.J. Messias and L. Memery for CFCs measurements has been greatly appreciated on board and particularly the long work of J.F.Ternon who also participated to the final data validation.

This work was supported by ORSTOM (Institut Français de Recherche Scientifique pour le Développement en Coopération) and IFREMER (Institut Français de Recherche pour l'Exploitation de la MER). The program was part of the PNEDC (Programme National d'Etude de la Dynamique du Climat).

References

Andrié C, Ternon JF (1994) Mesures des chorofluorométhanes in: Campagne CITHER-1. Recueil de données, Volume 3/4: Traceurs géochimiques. Documents scientifiques N°OP.15 du Centre ORSTOM de Cayenne, 67-77

Bennekom AJ (1995) Silica signals in the South Atlantic, this issue.

Böning C, Schott F (1993) Deep currents and the eastward salinity tongue in the equatorial Atlantic: results from an eddy-resolving, primitive equation model. J Geophys Res 98:6991-6999

Bullister JL (1989) Chlorofluorocarbons as time-dependent tracers in the ocean. Oceanography nov.89:12-17

Bullister JL, Weiss RF (1988) Determination of CCl_3F and CCl_2F_2 in seawater and air. Deep-Sea Res 35:839-853

Le Groupe CITHER 1 (1994a) Campagne CITHER-1. Recueil de données. Volume 1/4: Mesures "en route", Courantométrie ADCP et PEGASUS. Documents scientifiques N°OP 14, Centre ORSTOM de Cayenne, 161 pp

Le Groupe CITHER 1 (1994b) Campagne CITHER-1. Recueil de données. Volume 2/4: CTD-O2. Rapport interne LPO 94-04, Laboratoire de Physique des Océans, Brest

Le Groupe CITHER 1 (1994c) Campagne CITHER-1. Recueil de données. Volume 3/4: Traceurs géochimiques (1). Documents scientifiques N°OP 15, Centre ORSTOM de Cayenne, 525 pp

Colin C, Bourlès B (1994) Western boundary currents and transports off French Guiana as inferred from Pegasus observations. Oceanologica-Acta 17: 143-157

Doney SC, Bullister JL (1992) A chlorofluorocarbon section in the eastern North Atlantic. Deep-Sea Res 39:1857-1883

Doney SC, Jenkins WJ (1994) Ventilation of the Deep Western Boundary Current and abyssal western North Atlantic: estimates from tritium and ^{3}He distributions. J Physical Oceanogr 24:638-659

Durrieu de Madron X, Weatherly G (1994) Circulation, transport and bottom boundary layers of the deep currents in the Brazil basin. J Mar Res 52:583-638

Fine RA, Molinari RL (1988) A continuous deep western boundary current between Abaco (26,5°N) and Barbados (13°N). Deep-Sea Res 35:1441-1450

Fine RA, Warner MJ, Weiss RF (1988) Water mass modification at the Agulhas Reteroflection: chlorofluoromethane studies. Deep-Sea Res 35:311-332

Friedrichs MAM (1992) Meridional circulation in the tropical North Atlantic. Master's Thesis, MIT/WHOI, 88 pp

Friedrichs MAM, Hall MM (1993) Deep circulation in the tropical North Atlantic. J Mar Res 51:697-736

Friedrichs MAM, McCartney MS, Hall MM (1994) Hemispheric asymmetry in the vertical structure of Atlantic deep waters. J Geophys Res 99:25165-25179

Johns WE, Fratantoni DM, Zantopp RJ (1993) Deep western boundary current variability off northeastern Brazil. Deep-Sea Res 40:293-310

Kawase M (1993) Topographic effects on the bottom water circulation of the western tropical north Atlantic ocean. Deep-Sea Res 40:1259-1283

Kawase M, Sarmiento JL (1986) Circulation and nutrients in middepth Atlantic waters. J Geophys Res 91:9749-9770

Kawase M, Rothstein LM, Spriinger SR (1992) Encounter of a deep western boundary current with the equator: a numerical spin-up experiment. J Geophys Res 97:5447-5463

McCartney MS (1993) Crossing of the equator by the Deep Western Boundary Current in the Western Atlantic Ocean. J Phys Oceanogr 23:1953-1974

McCartney MS, Bennett SL, Woodgate-Jones ME (1991) Eastward flow through the Mid-Atlantic Ridge at 11°N and its influence on the abyss of the eastern basin. J Phys Oceanogr 21:1089-1121

McCartney MS, Curry RA (1993) Transequatorial flow of Antarctic bottom water in the western Atlantic ocean: abyssal geostrophy at the equator. J Phys Oceanogr 23:1264-1276

Messias MJ (1994) Les chlorofluoromethanes, traceurs des eaux profondes dans les zones de fracture Romanche et Chain en Atlantique équatorial. Thesis, Université Paris 6

Molinari RL, Fine RA, Johns E (1992) The Deep Western Boundary Current in the tropical North Atlantic Ocean. Deep-Sea Res 39:1967-1984

Pickart RS (1992) Water mass components of the North Atlantic deep western boundary current. Deep-Sea Res 39:1553-1572

Pickart RS, WM Smethie Jr. (1993) How does the deep western boundary current cross the Gulf Stream? J Phys Oceanogr 23: 2602-2616

Pickart RS, Hogg NG, Smethie WM (1989) Determining the strength of the deep western boundary current using the chlorofluoromethane ratio. J Phys Oceanogr 19:940-951

Ponte RM, Luyten J, Richardson PL (1990) Equatorial deep jets in the Atlantic ocean. Deep-Sea Res 37:711-713

Reid JL(1994) On the total geostrophic circulation of the North Atlantic ocean: flow patterns, tracers, and transports. Progr Oceanogr 33:1-92

Rhein M (1991) Ventilation rates of the Greenland and Norwegian seas derived from distributions of the chlorofluoromethanes F11 and F12. Deep-Sea Res 38:485-503

Rhein M (1994) The Deep Western Boundary Current: tracers and velocities. Deep-Sea Res 41: 263-281

Rhein M, Stramma L, Send U (1995) The Atlantic Deep Western Boundary Current: water masses and transports near the equator. J Geophys Res 100:2441-2457

Richardson PL, Schmitz Jr WJ (1993) Deep cross-equatorial flow in the Atlantic measured with SOFAR floats. J Geophys Res 98:8371-8387

Schott F, Fisher J, Reppin J, Send U (1993) On mean and seasonal currents and transports at the western boundary of the equatorial Atlantic. J Geophys Res 98:14353-14368

Smethie Jr W (1993) Tracing the thermohaline circulation in the western North Atlantic using chlorofluorocarbons. Progr Oceanogr 31:51-99

Speer KG, McCartney MS (1991) Tracing lower north Atlantic deep water across the equator. J Geophys Res 96:443-448

Talley LD, Johnson GC (1994) Deep, zonal subequatorial currents. Science 263:1125-1128

Tsuchiya M, Talley LD, McCartney MS (1992) An

eastern Atlantic section from Iceland southward across the equator. Deep-Sea Res 39:1885-1917
Tsuchiya M, Talley LD, McCartney MS (1994) Water-mass distributions in the western South Atlantic; a section from South Georgia Island (54S) northward across the equator. J Mar Res 52:55-81
Wallace DWR, Beining P, Putzka A (1994) Carbon tetrachloride and chlorofluorocarbons in the South Atlantic Ocean, 19°S. J Geophys Res 99:7803-7819
Wallace DWR, Lazier JRN (1988) Anthropogenic chlorofluoromethanes in newly formed Labrador sea water. Nature 332:61-63
Warner MJ, Weiss RF (1985) Solubilities of chlorofluorocarbons 11 and 12 in water and seawater. Deep-Sea Res 32:1485-1497
Weiss RF, Bullister JL, Gammon RH, Warner MJ (1985) Atmospheric chlorofluoromethanes in the deep equatorial Atlantic. Nature 314:608-610
Weiss RF, Warner MJ, Harrison KG, Smethie WM (1989) Deep equatorial Atlantic chlorofluorocarbon distributions. EOS, Trans American Geophysical Union 70:1132
Weisse R, Mikolajewicz U, Maier-Reimer E (1994) Decadal variability of the North Atlantic in an ocean general circulation model. J Geophys Res 99:12411-12421

Reprint from:

The South Atlantic

Present and Past Circulation

Edited by Gerold Wefer, Wolfgang H. Berger, Gerold Siedler, David J. Webb

ISBN 3-540-62079-6

LED - ED - DP